

Reactivation of sub-bandgap absorption in chalcogen-hyperdoped silicon

Bonna K. Newman,¹ Meng-Ju Sher,^{2,a)} Eric Mazur,^{2,3} and Tonio Buonassisi¹

¹Massachusetts Institute of Technology, Cambridge, Massachusetts 02139, USA

²Department of Physics, Harvard University, 9 Oxford Street, Cambridge, Massachusetts 02138, USA

³School of Engineering and Applied Sciences, Harvard University, 9 Oxford Street, Cambridge, Massachusetts 02138, USA

(Received 22 December 2010; accepted 20 May 2011; published online 21 June 2011)

Silicon doped with nonequilibrium concentrations of chalcogens using a femtosecond laser exhibits near-unity absorption of sub-bandgap photons to wavelengths of at least 2500 nm. Previous studies have shown that sub-bandgap absorptance decreases with thermal annealing up to 1175 K and that the absorption deactivation correlates with chalcogen diffusivity. In this work, we show that sub-bandgap absorptance can be reactivated by annealing at temperatures between 1350 and 1550 K followed by fast cooling (>50 K/s). Our results suggest that the defects responsible for sub-bandgap absorptance are in equilibrium at high temperatures in hyperdoped Si:chalcogen systems. © 2011 American Institute of Physics. [doi:10.1063/1.3599450]

Hyperdoping silicon with heavy chalcogens (sulfur, selenium, or tellurium) to orders of magnitude above room-temperature solubility results in strong sub-bandgap absorptance to at least 2500 nm.^{1,2} Hyperdoped silicon has potential use in infrared detectors,³ light emitting diodes,⁴ and a wide range of other semiconductor devices.⁵ However, the exact mechanism for the enhanced broadband absorptance is not yet well understood.

Previous research demonstrated that thermal annealing of hyperdoped silicon decreases absorption of photons with energy less than the bandgap.^{1,6} The sub-bandgap absorptance decreases with increased annealing time and temperature up to 1175 K. After annealing, the sub-bandgap absorptance is a function of dopant diffusion lengths, regardless of the dopant species (S, Se, or Te).⁶ It was suggested that precipitation of supersaturated dopant species at heterogeneous nucleation sites, such as grain boundaries, may cause the deactivation of the sub-bandgap absorptance.⁶

In this letter, we probe the thermodynamics of sub-bandgap absorptance at higher temperatures and observe a behavior not predicted by the previously proposed diffusion/precipitation model. Thermal annealing at temperatures above 1350 K followed by rapid cooling maintains sub-bandgap absorptance in hyperdoped silicon for both sulfur and selenium dopants. We also show that the fraction of sub-bandgap photons absorbed depends on the cooling rate, suggesting a kinetically limited process. Furthermore, sub-bandgap absorptance is reactivated in samples where it has previously been deactivated by annealing. In addition to offering insight into the nature of the sub-bandgap absorptance in hyperdoped silicon, these results demonstrate that the sub-bandgap absorptance can be thermally engineered and controlled to optimize device characteristics and performance, increasing the practical applications of chalcogen-hyperdoped silicon.

To explore the high-concentration, high-temperature regime of the Si:chalcogen system, we hyperdoped a set of c-Si samples with sulfur and selenium using a femtosecond laser doping technique, detailed elsewhere.^{1,2,6} We used

boron-doped silicon (100) wafers ($\rho > 100 \Omega \text{ cm}$). For sulfur doping, the wafer is placed on a translation stage in a chamber filled with sulfur hexafluoride (SF_6) gas to 6.7×10^4 Pa. For selenium doping, we thermally evaporate a thin 65 nm selenium film (99.95% purity) onto the wafer before loading the sample into the chamber filled with nitrogen to 6.7×10^4 Pa. We irradiate the wafers with 80 fs, 800 nm Ti:sapphire laser pulses. The laser pulses have average energy of 1.7 mJ and are focused to $420 \mu\text{m}$ (full width at half maximum of a Gaussian intensity profile) to achieve a fluence of 8 kJ/m^2 for sulfur doping and to $590 \mu\text{m}$ (yielding a fluence of 4 kJ/m^2) for selenium doping. A $20 \times 40 \text{ mm}^2$ area is irradiated by translating the sample stage at 1.2 mm/s. After laser irradiation, the surface layer of the silicon wafer is heavily doped with sulfur or selenium with concentrations between 10^{20} and 10^{21} cm^{-3} .² The surface is transformed into a rough landscape of micrometer-scaled spikes. The formation and structural characteristics of these spikes are discussed elsewhere.⁷ As a control sample, we laser irradiated silicon without dopant precursor in a nitrogen environment.

After laser doping, samples were cut into $5 \times 5 \text{ mm}^2$ squares for annealing in a vertical tube furnace at a temperature between 1070 and 1600 K. We annealed each sample separately on a clean quartz sample holder and measured the temperature with an R-type thermocouple located at the same height. After 30 min, the sample was cooled in one of three ways: dropped into silicone oil for fast quenching (250 K/s); removed from the furnace and air quenched on the quartz sample holder (50 K/s); or cooled in a controlled manner inside the furnace at 0.25 K/s to room temperature. To test reversibility of the thermal treatments, we annealed two Si:S samples at 1070 K for 30 min, and then performed a second thermal treatment. The second thermal treatment consisted of either a higher temperature furnace anneal at 1510 K or a second laser irradiation with the same parameters as the first, but in a dopant-free environment.

After annealing, the spectrally dependent transmission (T) and reflection (R) was measured using a spectrophotometer with an integrating sphere. Absorptance is calculated as $A = 1 - R - T$. A sample that is not annealed exhibits near unity

^{a)}Electronic mail: sher@physics.harvard.edu.

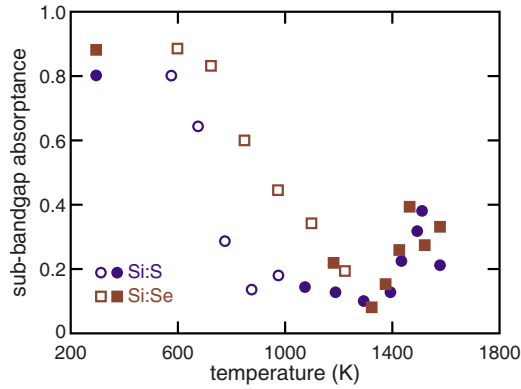


FIG. 1. (Color online) Average sub-bandgap absorbance for Si:S (circles) and Si:Se (squares) hyperdoped silicon after high-temperature anneals followed by oil quenching (250 K/s) for Si:S samples or air quenching (50 K/s) for Si:Se samples. Data points at 295 K are samples before annealing. Measurable increases in sub-bandgap absorbance occur at temperatures above 1350 K. Standard deviations of each data point is less than 0.05. Data points with unfilled symbols are from Refs. 6 (Si:S) and 15 (Si:Se).

absorbance from 400 to 2500 nm for both Si:S and Si:Se. For characterization, we average sub-bandgap absorbance from 1250 to 2500 nm. We estimate light scattering out of the integrating sphere to cause an overestimation of the absorbance by at most 0.07.

Figure 1 shows the average sub-bandgap absorbance of samples annealed between 1070 and 1600 K. For both Si:S and Si:Se, we observe enhancement of the sub-bandgap absorbance for samples annealed above 1350 K and then rapidly quenched. Samples annealed at higher temperatures exhibit stronger absorbance. However, as the temperature approaches 1550 K, the absorbance decreases. Scanning electron microscopy of the surface of these Si:Se samples suggests that local surface melting occurs during annealing. Redistribution of dopant atoms on the surface or dopant evaporation could explain the sudden drop in sub-bandgap absorbance.

We verified that enhanced sub-bandgap absorbance depends on the presence of the dopant atoms by performing a high-temperature anneal at 1490 K followed by quenching of two control samples: (1) a bare c-Si wafer that was not hyperdoped and (2) a sample irradiated with fs laser in a nitrogen environment, containing no dopant but exhibiting micrometer-scaled surface features. The bare c-Si wafer exhibits average sub-bandgap absorbance of 0.02 ± 0.01 after annealing and quench. Sub-bandgap absorbance of the nitrogen sample after annealing is measured at 0.10 ± 0.02 . Much of this measured sub-bandgap absorbance is likely due to light scattering effects, as noted above.

The amount of sub-bandgap absorbance depends on the cooling rate from high temperature. Figure 2 shows the results of cooling at different rates. The sample quenched at 250 K/s exhibits the largest average sub-bandgap absorbance (0.33 ± 0.01), followed by the sample quenched at 50 K/s (0.24 ± 0.02), and finally the sample that underwent controlled cooling at 0.25 K/s (0.14 ± 0.02).

Sub-bandgap absorbance is reactivated in samples where it was previously deactivated by annealing. We performed two-step anneals summarized schematically in Fig. 3. A Si:S sample was annealed at 1070 K for 30 min and quenched in air, resulting in an average sub-bandgap absorbance of 0.12 ± 0.01 . The same sample was then reannealed

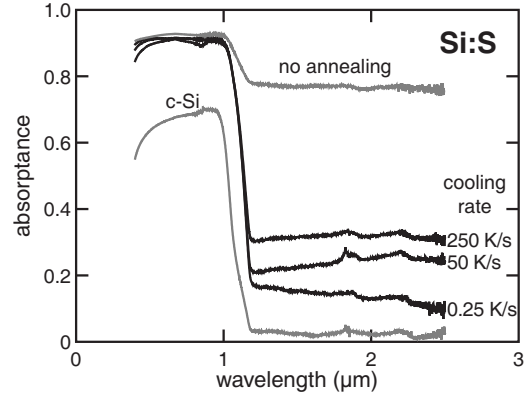


FIG. 2. Absorbance as a function of cooling rate for Si:S samples. Samples were annealed at 1490 K for 30 min. The cooling rates are derived from a one-dimensional convection model for cooling from 1520 to 1100 K in different media. Absorbance data of an untreated, crystalline silicon wafer and a Si:S sample prior to annealing are included for comparison.

at 1510 K for an additional 30 min followed by oil quench. We find that the average sub-bandgap absorbance increases to 0.24 ± 0.01 . A Si:S control sample, annealed only once at 1510 K, has an average sub-bandgap absorbance of 0.38 ± 0.02 .

The sub-bandgap absorbance is also reactivated by a second laser treatment, as seen in Fig. 3. Sub-bandgap absorbance of a Si:S sample was first deactivated by annealing at 1070 K for 30 min and was reactivated to 0.59 ± 0.04 after a second laser irradiation in a nitrogen environment. We compare this to a control sample that was laser-irradiated twice, first for hyperdoping and the second time with no dopant present and no anneal in between (average sub-bandgap absorbance = 0.60 ± 0.02). This corresponds to an almost complete restoration of the sub-bandgap absorbance. The slight decrease in absorbance for both samples after the second laser irradiation is likely due to loss of dopant atoms through laser ablation.

The results presented in this letter show that sub-bandgap absorbance is reactivated through high-temperature annealing. The amount of sub-bandgap absorbance depends on the rate of postanneal cooling, suggesting a kinetically limited deactivation process.

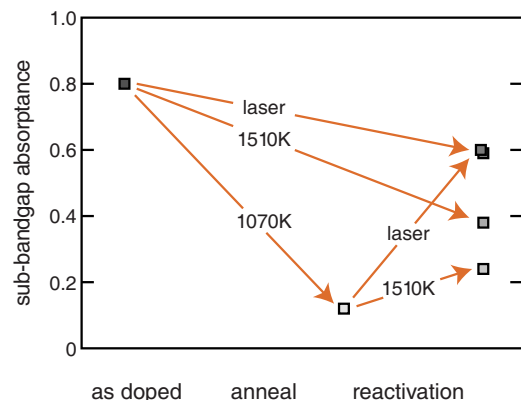


FIG. 3. (Color online) Schematic of the two-step annealing process that first deactivates the sub-bandgap absorbance by annealing at 1070 K and then reactivates it via one of two methods: high temperature (1510 K) annealing and quenching or laser irradiation. Control samples are also shown for comparison.

In the intermediate temperature regime, from 1070 to 1350 K, annealing followed by quenching results in deactivation of sub-bandgap absorptance in agreement with previous results of annealing followed by slow cooling, as seen in Fig. 1. If we correlate the sub-bandgap absorptance to the concentration of an optically active defect state, we note the similarities of the results in Fig. 1 to a time-temperature-transformation diagram describing the precipitation of supersaturated point defects at heterogeneous nucleation sites, as previously reported for Si:Fe.⁸ At lower temperatures, the precipitation of supersaturated point defects is energetically favorable but kinetically limited by diffusion. At higher temperatures, the equilibrium solubility of point defects increases with temperature.

The enhanced broadband absorptance of chalcogen-doped silicon is only observed in samples with supersaturated chalcogen concentrations, and the origin of the sub-bandgap absorption is not yet well understood. Chalcogen defect centers have been studied extensively in diffusion experiments; isolated substitutional impurities and dimer pairs are the most common point defects, and other more complex defect centers have been identified.^{9,10} These known defect centers introduce deep states that allow sub-bandgap photon absorption, however, in samples with chalcogen dopant concentrations up to $7 \times 10^{16} \text{ cm}^{-3}$, no significant broadband, sub-bandgap absorptance has been reported.^{11,12} In femtosecond-laser chalcogen-hyperdoped silicon studied in this letter, the initial dopant concentration² is at least 1000 times larger than the high-temperature equilibrium solubility achieved via solid-state thermal diffusion from a chalcogen-rich surface source: $3 \times 10^{16} \text{ cm}^{-3}$ for S and $2 \times 10^{17} \text{ cm}^{-3}$ for Se.^{13,14} Our results suggest that a point defect state associated with higher concentrations of chalcogen dopant atoms and with unique optical characteristics is stable at temperatures higher than 1350 K in these samples. Further structural studies to identify this chemical state are underway.

High-temperature annealing followed by quenching of silicon hyperdoped with sulfur or selenium results in the re-activation of sub-bandgap optical absorptance that is not explained by previous models. Sub-bandgap absorptance is maintained in hyperdoped samples annealed above 1350 K and cooled at rates faster than 50 K/s. A high concentration

of point defects stable at high temperatures may be responsible for absorption of sub-bandgap photons. Our results demonstrate an ability to control sub-bandgap absorptance in Si:chalcogen-hyperdoped systems using thermal processing.

Several people contributed to the work described in this letter. T.B. conceived of the basic idea for this work. B.K.N. and M.S. contributed equally; they performed the experiments and prepared the manuscript. E.M. and T.B. supervised the research. The authors are very grateful for helpful discussions with Alison Greenlee and Elena Read. The research described in this letter was supported by Chesonis Family Foundation, and the National Science Foundation under Contract Nos. CBET 0754227 and CHE-DMR-DMS 0934480. B.K.N. acknowledges support of the Clare Boothe Luce Foundation.

¹C. H. Crouch, J. E. Carey, M. Shen, E. Mazur, and F. Y. Genin, *Appl. Phys. A: Mater. Sci. Process.* **79**, 1635 (2004).

²M. A. Sheehy, B. R. Tull, C. M. Friend, and E. Mazur, *Mater. Sci. Eng., B* **137**, 289 (2007).

³J. E. Carey, C. H. Crouch, M. Y. Shen, and E. Mazur, *Opt. Lett.* **30**, 1773 (2005).

⁴J. M. Bao, M. Tabbal, T. Kim, S. Charnvanichborikarn, J. S. Williams, M. J. Aziz, and F. Capasso, *Opt. Express* **15**, 6727 (2007).

⁵A. Serpenguezel, A. Kurt, I. Inanc, J. E. Cary, and E. Mazur, *J. Nanophotonics* **2**, 021770 (2008).

⁶B. R. Tull, M. T. Winkler, and E. Mazur, *Appl. Phys. A: Mater. Sci. Process.* **96**, 327 (2009).

⁷B. R. Tull, J. E. Carey, E. Mazur, J. P. McDonald, and S. M. Yalisove, *MRS Bull.* **31**, 626 (2006).

⁸W. B. Henley and D. A. Ramappa, *J. Appl. Phys.* **82**, 589 (1997).

⁹H. G. Grimmeiss and E. Janzen, in *Deep Centers in Semiconductors*, edited by S. T. Pantelides (Gordon and Breach, New York, 1992), p. 89.

¹⁰A. A. Taskin and E. G. Tishkovskii, *Semiconductors* **36**, 605 (2002).

¹¹N. Sclar, *J. Appl. Phys.* **52**, 5207 (1981).

¹²N. S. Zhdanovich and Y. I. Kozlov, *Sov. Phys. Semicond.* **10**, 1102 (1976).

¹³R. O. Carlson, R. N. Hall, and E. M. Pell, *J. Phys. Chem. Solids* **8**, 81 (1959).

¹⁴H. R. Vydyanath, J. S. Lorenzo, and F. A. Kroger, *J. Appl. Phys.* **49**, 5928 (1978).

¹⁵B. K. Newman, J. T. Sullivan, M. Winkler, M. J. Sher, M. A. Marcus, S. Fakra, M. J. Smith, S. Gradecak, E. Mazur, and T. Buonassisi, Proceedings of the 24th European Photovoltaic Solar Energy Conference, Hamburg, Germany, 2009, p. 236.